

Dapagliflozin improves early diabetic nephropathy by downregulating PPP2R2A and CXCL12/S100A13 through ROS- dependent

Wang Suhong

Second Hospital of Jilin University

Yang Maoguang

Second Hospital of Jilin University

Cheng Yan

Second Hospital of Jilin University

Ning Lili

Second Hospital of Jilin University

Li Mo

Second Hospital of Jilin University

Yan Yan

Second Hospital of Jilin University

Shen Hong

Second Hospital of Jilin University

Cai Hanqing (✉ caihanqing16@163.com)

Second Hospital of Jilin University

Research Article

Keywords: Diabetic nephropathy, type 2 diabetes, SGLT2i, proteomics, signaling pathways, molecular mechanisms

Posted Date: May 10th, 2022

DOI: <https://doi.org/10.21203/rs.3.rs-1511213/v1>

License:   This work is licensed under a Creative Commons Attribution 4.0 International License. [Read Full License](#)

Abstract

Diabetic nephropathy (DN) is a common chronic complication of diabetes mellitus (DM), and dapagliflozin, a representative drug of sodium-glucose co-transport protein 2 inhibitors (SGLT2i), is a novel hypoglycemic agent for the treatment of type 2 diabetes mellitus (T2DM), which has been shown to reverse microalbuminuria in early type 2 diabetic nephropathy (T2DN), but the mechanism of action remains to be elucidated. In this study, five patients with early T2DN treated in our hospital from October 2020 to May 2021 were selected for the study and were treated with insulin combined with dapagliflozin to lower glucose, and the initial insulin treatment was named as DN group, and the addition of dapagliflozin was named as DN-DAPA group, and another five patients with a healthy physical examination at the same period were selected as the blank control group (NC group). Patients' morning urine samples were collected and processed using iTRAQ unlabeled quantitative proteomics technology. Bioinformatics analysis was performed to obtain 193 differentially expressed proteins. 91 expressions were up-regulated and 72 expressions were down-regulated in the DN group compared with the NC group, and 11 expressions were up-regulated and 26 expressions were down-regulated in the DN-DAPA group compared with the DN group. Five significantly co-expressed protein molecules were screened at $P < 0.05$ and $[\log_{2}FC] > 1.5$: SOD1, SLC25A6, S100A13, PPP2R2A, CXCL12. Therefore, these differential proteins are associated with early T2DN injury. Molecularly, dapagliflozin improves mitochondrial oxidative stress and reduces urinary microalbumin excretion in early T2DN patients by inhibiting PPP2R2A and CXCL12/ S100A13 pathways to reverse early T2DN.

1. Introduction

The International Diabetes Federation announced that approximately 463 million people will have diabetes mellitus (DM) in 2019, and this number will increase by 25% in 2030 and by 51% in 2045 ^[1]. It is estimated that about 20–40% of patients with DM develop DN (Diabetic Nephropathy, DN) ^[2]. DN is a major cause of end-stage renal failure and chronic kidney disease ^[3] and a major contributor to death in patients with DM ^[4]. According to the Mogensen staging method, there are five stages of DN ^[5], and stages I-III are the early stages of DN, which can be reversed with active and effective treatment. It is urgent to find the pathogenesis of DN as well as safe and effective therapeutic targets and timely intervention.

Sodium-Glucose Cotransporter-2 Inhibitors (SGLT-2i) is a new class of drugs approved for the treatment of T2DM. Dapagliflozin, a representative drug of SGLT2i. SGLT-2i not only lowers blood glucose to improve metabolism, but also may improve hemodynamics ^[6], reduce body weight ^[7], it may play a role in protecting the kidney and reducing microalbuminuria by improving vascular endothelial function ^[8], restoring tubulobulb feedback, reducing glucotoxicity ^[9], reducing the inflammatory response and fibrosis ^[10], and reducing proximal tubular cell ^[11] hyperfiltration, among other mechanisms to delay the decline of glomerular filtration rate, and has been confirmed in several large prospective trials ^[12–14].

Studies ^[15, 16] have shown that the overall proteome of DN patients is altered before significant pathological changes occur in the kidney. A comprehensive study of the urinary proteome in DN patients

can provide a timely and intuitive understanding of the development of the disease and the molecular mechanism of SGLT-2i to improve early DN and obtain potential therapeutic targets of the disease, laying the foundation for early diagnosis and treatment. Based on the proteomics research technology, this paper investigates two aspects of T2DN pathogenesis and the molecular mechanism of dapagliflozin action.

2. Subjects And Methods

2.1. Study subjects and grouping

The study was a single-center retrospective cohort study in which five patients with mild to moderate T2DN who attended the Second Hospital of Jilin University from October 2020 to May 2021 were selected, and five patients met all inclusion and exclusion criteria (Table 1). Morning clean middle urine samples were collected from 5 patients who applied insulin therapy only, and the samples were named as DN group. For the above 5 patients treated with dapagliflozin for more than 12 weeks, morning clean mid-section urine samples were collected again and named as DN-DAPA group; another 5 cases of healthy people in the same period were selected as a blank control group and named as NC group.

Baseline and follow-up information was collected from all study subjects, including data on patient gender, age, disease duration, height, weight, abdominal circumference, and BMI. Fasting glucose, fasting C-peptide, 1h postprandial C-peptide, 2h postprandial C-peptide, glycosylated hemoglobin (Hemoglobin A1c, HbA1c), total cholesterol (TC), triglyceride (TG), low-density lipoprotein cholesterol (LDL-C), and high-density lipoprotein cholesterol (HDL-C) were also recorded before and after dapagliflozin administration. lipoprotein cholesterol (LDL-C), high-density lipoprotein cholesterol (HDL-C), serum creatinine (Scr), uric acid (UA), urine microalbumin Creatinine ratio (ACR), glomerular filtration rate (eGFR), and other biochemical indicators.

This study is in accordance with the Declaration of Helsinki. It was reviewed and approved by the Ethics Committee of the Second Hospital of Jilin University.

2.2 Collection and analysis of urine samples

Samples were collected from mid-morning urine using standard consistent procedures and stored at -80°C. Samples were removed from -80°C, melted completely, vortexed, and mixed thoroughly, and a volume of 8 M urea-complexed protein was added for protein concentration determination using the BCA kit. Equal amounts of each sample protein were digested, and the volume was adjusted to the same level with lysate, then dithiothreitol (DTT) was added to a final concentration of 5 mM and reduced at 56 °C for 30 min. Iodoacetamide (IAA) was added to a final concentration of 11 mM and incubated for 15 min at room temperature and protected from light. TEAB was added to dilute urea to ensure that the concentration was below 2 M. A ratio of 1:50 (protease Add trypsin at a ratio of 1:50 (protein, m/m) and digest overnight. Trypsin was added at a ratio of 1:100 (protease: protein, m/m) and the digestion was continued for 4 h.

2.3 Liquid chromatography-mass spectrometry (LC-MS/MS) coupled analysis

The peptides were separated by a UHPLC system and injected into an NSI ion source for ionization and then into an Orbitrap Exploris™ 480 mass spectrometer for analysis. The ion source voltage is set to 2.3 kV and the FAIMS compensation voltage (CV) is set to -45V,-65V. The peptide parent ions and their secondary fragments are detected and analyzed using a high-resolution Orbitrap. The primary mass spectrometry scan range was set to 400 - 1200 m/z and the scan resolution was set to 60000; the secondary mass spectrometry scan range was set to a fixed starting point of 110 m/z, the secondary scan resolution was set to 15000, and TurboTMT was set to Off. The data acquisition mode was performed using a Cycle time-based data-dependent scanning (DDA) program, and the same sequential secondary mass spectrometry was analyzed. To improve the effective utilization of the mass spectrum, the automatic gain control (AGC) was set to 100%, the signal threshold was set to 5E4 ions/s, the maximum injection time was set to Auto, and the dynamic exclusion time of the tandem mass spectrometry scan was set to 20 s to avoid repeated scanning of the parent ions.

2.4 Database search

Secondary mass spectrometry data were retrieved using Proteome Discoverer (v2.4.1.15). The search parameters were set: the database was

Homo_sapiens_9606_SP_20201214.fasta (20395 sequences), an inverse library was added to calculate the false positive rate (FDR) due to random matching, and a common contamination library was added to the database to eliminate the effect of contaminated proteins in the identification results; the digestion method was set to Trypsin (Full); the number of missed cut sites was set to 2; the minimum peptide length was set to 6 amino acid residues; the maximum number of peptide modifications was set to 3; the mass error tolerance of primary parent ion was set to 10 ppm, and the mass error tolerance of secondary fragment ion was set to 0.02 Da. Carbamidomethyl (C) was set as fixed modification, Oxidation (M), and Acetyl (N-terminus), Met-loss (M), Met-loss+acetyl (M), and deamidation (NQ) were set as variable modifications. The FDR for protein, peptide, and PSM identification were all set to 1%.

2.5 Bioinformatics analysis

The identified differential proteins were GO-annotated using eggno-mapper software (v2.0), and the GO ID of each protein annotation result was extracted, and then the proteins were functionally classified according to Cellular Component (CC), Biological Process (BP), and Molecular Function (MF) to classify the proteins functionally. Then, we annotated the protein pathways based on the KEGG pathway database, and the identified proteins were subjected to BLAST comparison (blastp, $evalue \leq 1e-4$), and for each sequence, the comparison result with the highest score (score) was selected for annotation.

The information on functional categories enriched to all protein groupings and the corresponding enriched P-values were first collected, and then the functional categories that were significantly enriched ($P < 0.05$) in at least one protein grouping were screened. The filtered P-value data matrix was first log-transformed by $-\log_{10}$, and then the transformed data matrix was Z-transformed for each functional category. The data set obtained after Z-transformation was subjected to one-sided cluster analysis using the hierarchical

clustering (Euclidean distance, mean linkage clustering) method. The clustering relationships are visualized using a heat map drawn using the function heatmap.2 in the R language package gplots.

2.6 Statistical methods

SPSS 25 software was used for statistical analysis. Measures obeying normal distribution were statistically described using mean \pm standard deviation ($X \pm S$); measures not obeying normal distribution were statistically described using median and interquartile spacing, and differences between groups were compared using the t-test. The statistical analysis of frequency was used to represent the count data, and the X test was used for the difference between groups.

Conditions for screening differential proteins: the relative quantitative values of each protein in the two comparison groups of samples were subjected to T-test and the corresponding P-value was calculated as an indicator of significance, with the default $P \leq 0.05$. The relative quantitative values of proteins were log₂ log-transformed before the test so that the test data conformed to the normal distribution required for the t-test, and then the P-value was calculated using a two-sample two-tailed t-test. $p \leq 0.05$ and $|\log FC|$; (fold change) > 1.5 was considered statistically significant. When $P < 0.05$, differential expression change > 1.5 was the threshold of change for significant upregulation, and $< 1/1.5$ was the threshold of change for significant downregulation.

3. Results

3.1 General Information

The clinical and biochemical characteristics of the study subjects are shown in Table 2. 1 of the 5 patients was in Mogensen stage III and 4 patients were in stage II. BMI, HbA1c%, FPG, Scr, SBP, DBP, and eGFR were higher in the DN and DN-DAPA groups than in the healthy subject's group (NC group). UA, TC, TG, and LDL were higher in the NC group than in the DN group. Among them, only the change in HbA1c% was statistically significant ($p < 0.05$).

3.2 Screening of differentially expressed proteins

After normalization of the data, with differential expression $|\log_2 FC| > 1.5$ as the threshold of change and $P < 0.05$, a total of 193 differential proteins were detected (Figure 1). We focused on the proteins with opposite expression trends in the DN/NC and DN-DAPA/DN groups and obtained a total of 7 protein molecules, of which only one protein molecule, PLEKHB2, was down-regulated in the DN/NC group and up-regulated in the DN-DAPA/DN group, while the remaining 6 protein molecules were up-regulated in the DN/NC group and down-regulated in the DN-DAPA/DN group. The remaining six proteins were up-regulated in the DN/NC group and down-regulated in the DN-DAPA/DN group. By searching DN-related literature, five of the differential proteins closely related to DN were selected (Table 3): SOD1, SLC25A6, PPP2R2A, S100A13, CXCL12 for further analysis.

3.3 Functional classification and subcellular structural localization of differentially expressed urinary protein GO

According to gene ontology, the GO ID of each protein annotation result was extracted using eggno-mapper software (v2.0), and the proteins were classified by cellular component (CC), molecular function (MF), and biological function (BP) for GO function [17] and subcellular structure localization (Figure 2-3). These processes are important for further understanding of the proteins involved in DN progression and the mechanism of action of dapagliflozin on DN.

The differential proteins in DN/NC group and DN-DAPA/DN group have a similar functional classification, according to BP, more than 50% of up-and down-regulated proteins have a regulatory cellular process, biological regulation, metabolic process, response to stimulus function. The majority of differential proteins in MF have binding and catalytic acting activity functions (Figure 2A-B, Figure 3A-B). According to the subcellular localization, only CXCL12 was located in the extracellular, while SOD1, S100A13, PPP2R2A, and SLC25A6 were located in the cytoplasm.

3.4 GO enrichment analysis of differentially expressed proteins

To further analyze the possible functions of these differentially expressed proteins, the enrichment test was applied using Fisher's exact test, and the P values obtained are presented through bubble plots for the top 20 functional classifications in which differentially expressed proteins were significantly enriched ($P < 0.05$). The analysis resulted in a total of 28 biological process items, 16 cellular composition items, and 16 molecular function items (Figures 4-5).

The five differential proteins screened in this study were upregulated in expression in the DN/NC group. sLC25A6 in this comparative group is involved in the regulation of defense response of BP, CXCL12, SOD1, and S100A13 are involved in the extracellular space of CC. SOD1 is involved in the MF catalytic activity, acting on a protein function.

The above-mentioned differential proteins were changed after dapagliflozin application, with down-regulated expression in DN-DAPA/DN and altered GO functional enrichment to perform more biological functions. In BP enrichment analysis circulatory system development, positive regulation of cell growth regulation of cell growth, Cardiovascular system development functions are regulated by CXCL12, intermediate filament cytoskeleton organization, sensory organ development, negative regulation of lipid metabolic process, epithelial cell differentiation function is regulated by SOD1, SLC25A6 plays mitochondrion organization function, CSCL12 and SLC25A6 together play regulation of secretion by cell function. It can be seen that differentially expressed proteins are involved in more biological processes after the application of dapagliflozin, mostly focusing on the regulation of cell structure, growth, and development, differentiation, and secretion.

Cardiovascular system development functions are regulated by CXCL12, intermediate filament cytoskeleton organization, sensory organ development, negative regulation of lipid metabolic process, epithelial cell differentiation function is regulated by SOD1, SLC25A6 plays mitochondrion organization

function, CSCL12 and SLC25A6 together play regulation of secretion by cell function. It can be seen that differentially expressed proteins are involved in more biological processes after the application of dapagliflozin, mostly focusing on the regulation of cell structure, growth, and development, differentiation, and secretion.

In MF analysis, SLC25A6 plays an active transmembrane transporter activity function, PPP2R2A and SOD1 together form protein phosphatase binding as well as phosphatase binding, SOD1, and S100A13 SOD1 and S100A13 have the function of copper ion binding.

3.5 Enrichment analysis of differentially expressed protein KEGG signaling pathway

The KEGG pathway database^[18] was used to enrich the 2 comparative groups of differential protein pathways, and up-and down-regulated differential proteins were enriched to a total of 22 signaling pathways (Figure 6). The results showed that the top three pathways significantly enriched in DN/NC group and DN-DAPA/DN group for down-regulated proteins were: has05022, hsa05016, and hsa05020. according to the signaling pathway map, SOD1 and SLC25A6 were involved in three signaling pathways, and SOD1 could act directly or indirectly on SLC25A6 located in mitochondria.

4. Discussion

In this paper, we analyzed the molecular mechanism of reversal of microalbuminuria in early DN based on a proteomic approach with dapagliflozin. GO and KEGG pathway analysis of the differential proteins confirmed that mitochondrial energy metabolism, humoral immunity, and inflammation play key roles in DN kidney injury. The five screened differential proteins might be used as potential biological markers for DN.

Oxidative stress is closely related to DM and its complications^[19, 20] and plays an important role in the development of DN and its progression to end-stage renal disease^[21, 22]. Oxidative stress is directly associated with podocyte injury, proteinuria, and tubulointerstitial fibrosis^[23], and is associated with altered renal hemodynamics^[24], and has a synergistic effect. Reactive oxygen species (ROS) concentrations can reflect the level of oxidative stress in vivo. Physiological concentrations of ROS can play a role in signal transduction^[25], redox signaling pathways, and maintain intracellular homeostasis; low to moderate concentrations of ROS are beneficial for cell survival, stem cell function, and lifespan extension^[26, 27]; excess ROS damage cells by unbalancing the body's oxidative and antioxidant systems^[28], causing DNA, protein, and lipid damage and acting as signaling molecules in a variety of cellular damage pathways^[29-34]. Reducing excess ROS has been shown to slow the progression of various DM complications^[35-38]. Therefore, inhibition of ROS production may be beneficial in the treatment of DN. there are many pathways of ROS production in DM patients^[39], mainly during mitochondrial respiration^[40, 41]. Excessive ROS production is associated with mitochondrial dysfunction, so ROS is considered a biomarker of mitochondrial dysfunction in DN^[42-44]. Reduced mitochondrial ATP production, low levels of mitochondrial membrane potential (MMP), and increased mitochondrial debris are associated with tubular

cell injury and apoptosis in DN [45, 46]. Chronic hyperglycemia can also trigger mitochondrial fragmentation and promote mitochondrial dysfunction, as evidenced by elevated mitochondrial ROS production [47–49], increased mitochondrial permeability transition pore (mPTP) opening by pro-apoptotic factor leakage, and caspase-9 apoptotic pathway activation, etc. [50].

The present study hypothesized that dapagliflozin could restore mitochondrial function and exert anti-oxidative stress effects, as a link between SGLT2i and mitochondrial function has been previously reported [51–53]. The first line of defense against ROS-induced damage is the antioxidant enzyme SOD [54], of which SOD1 is the key enzyme of DN. SOD1 accounts for 85% of the total SOD activity in most mammalian cells [55] and is present in the cytoplasm, nucleus, peroxisomes, and mitochondria [56]. It can be used to scavenge superoxide anion radicals in organisms [57], and the excessive production of superoxide anions leads to the formation of secondary reactive oxygen species such as peroxynitrite and hydroxyl radicals. By activating PI3K/Akt signaling pathway, antioxidant drugs can increase SOD1 expression activity, enhance cellular antioxidant capacity, and mitigate oxidative damage, thus effectively preventing and controlling cellular DNA oxidative damage and mitochondrial dysfunction [58].

Several animal studies [55, 59, 60] and one study with DN patients [61] showed that SOD1 expression is downregulated in DN, unfortunately, none of these studies specified the stage of DN in which the subjects were studied. DeRubertis F R et al [62] showed that SOD1-deficient animal models can accelerate renal pathology. Recently Rodrigues A M et al [63] found that SOD1 expression was upregulated in an animal model of Wistar rats as an adaptive response to oxidative stress. Supplementation of SOD1 suppressed proteinuria and improved renal lesions [55], suggesting that the severity of DN could be reduced by upregulating SOD1 activity [64, 65], which is consistent with our findings. Unlike previous studies on SOD1, the present study for the first time specified the DN stage in which the study subjects were in Mogensen stages I-III, and the results showed that SOD1 protein expression was upregulated in the DN group compared with the NC group ($\log_2 F_c = 10.0041$, $p < 0.05$), while in the DN-DANA/DN group, dapagliflozin restored or changed the protein level toward healthy control (NC group) levels. Previous studies have differed for the expression levels of SOD1 in DN, and we speculate that the possible reasons are: 1) SOD1 is involved in the development of DN and the levels change dynamically throughout DN disease. 2) SOD1 is upregulated in response to increased oxidative stress, which is a key cellular defense mechanism against excessive oxidative stress. More studies are still needed to clarify the changes of SOD1 protein expression content in different DN stages.

CXCL12 is a chemokine and tissue repair marker widely expressed in multiple organs, highly active under pathological conditions such as inflammation [66] and ischemia, and promotes stem cell regeneration and tissue repair. It has been reported [67] that CXCL12 has anti-oxidative stress effects, and the main receptor of CXCL12 is CXCR4 [68], and disruption of CXCR4 receptors in mice leads to increased endogenous ROS production, and this study demonstrates for the first time that mitochondrial oxidative stress can be reduced through the CXCR4/CXCL12 axis, suggesting that the CXCR4/CXCL12 pathway in regulating intracellular ROS levels. To date, CXCL12 was always found in mice with six different splice variants [68], all

encoded by the CXCL12 gene. In contrast, only two isoforms, CXCL12 α and CXCL12 β , were found in humans [69], with more CXCL12 α than CXCL12 β . Therefore, we can assume that in the present study it was mainly CXCL12 α that played a role. CXCL12 α is recognized as a protective mediator of cell and tissue repair in DM and NDM kidney diseases [70, 71]. The results of the present study showed that CXCL12 expression was upregulated in the DN group compared to the NC group (log2Fc = 1.6263, P < 0.05), presumably because the organism is in the early stages of disease at this time with enhanced oxidative stress and foot cell damage, CXCL12 levels were upregulated as a protective mechanism, exerting anti-oxidative stress and reducing microalbuminuria. CXCL12 expression levels were gradually downregulated after dapagliflozin application (log2Fc = 1.8291, p < 0.05), presumably the mechanism of drug action was anti-oxidative stress. The reasons for the differences in the results of different studies may be related to different disease models and being indifferent DN stages, which still need to be further explored.

A recent study [72] showed that CXCR4 can maintain MMP and mitochondrial function through the JAK2/STAT3 pathway. STAT3 acts mainly as a transcription factor and is translocated into the nucleus after phosphorylation. STAT3 activation mediates the pathogenesis of DN [73]. Downregulation of CXCL12 α expression and reduced binding to CXCR4 will inhibit CXCL12 α / CXCR4 signaling and downstream STAT3S727 phosphorylation, impeding STAT3S727 translocation into mitochondria and ultimately leading to increased mitochondrial fragmentation and altered mitochondrial homeostasis. All of the above studies suggest that CXCL12 can be involved in regulating mitochondrial homeostasis directly or indirectly, regulating ROS levels and oxidative stress, etc.

There is an interaction between SOD1 and CXCL12 receptor CXCR4, and CXCL12 stimulation of cells overexpressing SOD1 is followed by a significant increase in Akt activation [74]. Several studies have shown that Akt is involved in the development of DM and its complications, such as the maintenance of normal glomerular endothelial cell function through the PIK3/Akt pathway [75], protection against high glucose-induced podocyte injury [76], and association with various cellular processes such as apoptosis, inflammation, and autophagy [77, 78]. In the present study, SOD1 was significantly more upregulated than CXCL12, which stimulates overexpression of SOD1 leading to increased Akt activation, and maybe a mechanism for improving early DN. The effect on SOD1 after application of dapagliflozin was greater than CXCL12, and the degree of SOD1 downregulation was significantly greater than CXCL12, and Akt activation was attenuated. We speculate that the reasons for this may be: 1) the application of dapagliflozin alleviates the renal oxidative stress damage induced by ROS, and the compensatory protection mechanism of the body is gradually weakened; 2) dapagliflozin directly mediates Akt activation through other signaling pathways other than CXCL12/SOD1 pathway.

SLC25A6, a member of the mitochondrial carrier subfamily, is commonly expressed in all tissues [79] and is a core component of mPTP. mPTP channels are a supramolecular complex of proteins in the outer and inner mitochondrial membranes and intermembrane spaces that are voltage- and Ca²⁺-dependent [80]. mPTP opening underlies the absence of mitochondrial membrane potential ($\Delta\psi_m$) and is involved in the cell apoptotic process [81]. Endoplasmic reticulum Ca²⁺ homeostasis is a key determinant of ROS levels and mPTP opening rate [82]. Based on the role of SLC25A6 [82] and the results of KEGG enrichment analysis, we

found that SLC25A6 is involved in this pathway of antioxidant defense system together with SOD1, which can regulate the expression level and function of mPTP by acting directly or indirectly on mPTP constructed with the participation of SLC25A6 and located upstream of SLC25A6 (see has05022, hsa05016, and hsa05020). In the early stage of DN development accompanied by elevated blood glucose, excessive ROS production leads the body to be under oxidative stress, while SCL25A6 expression is upregulated in the DN/NC group, so we hypothesized that the excessive ROS and upregulated SLC25A6 expression together activate mPTP, causing the kidney foot cells, thylakoid cells, etc. to swell and rupture, and the mitochondria located in the kidney to become dysfunctional or even cell-induced apoptosis. Combined with the previous paper, it is easy to find that SOD1 expression in DN-DAPA/DN group was significantly down-regulated after the application of dapagliflozin, the oxidative stress effect was gradually weakened, ROS production was reduced, SLC25A6 expression also became down-regulated, the degree of mPTP opening was reduced or even shut down, and the opening rate was reduced, which protected the kidney cells from oxidative stress damage. Therefore, we suggest that dapagliflozin exerts anti-oxidative stress and inhibits mitochondrial apoptosis, which is directly mediated through the inhibition of SOD1/SLC25A6 expression in renal cells. Combined with the interaction between the two and the subcellular structure localization, we infer that CXCL12 regulates SOD1/SLC25A6 extracellularly, so dapagliflozin may further inhibit SOD1/SLC25A6 by first acting on CXCL12 extracellularly to downregulate CXCL12 expression, but further experiments are needed to verify this.

S100A13 is a Ca^{2+} binding protein and belongs to the S100 protein family [83]. S100A13 protein is involved in Ca^{2+} homeostasis, energy metabolism, inflammation [84] and interacts with intracellular transcription factors and DNA, activating surfaces including RAGE and toll-like receptor 4, G protein-coupled receptors [85, 86]. It has been demonstrated that the receptor for S100A13 is the receptor for advanced glycosylation end products (RAGE), which is involved in inflammatory processes, plays a central role in acute and chronic inflammatory diseases, and is closely associated with DM complications [87]. S100 proteins act in an autocrine or paracrine manner after binding to RAGE [88, 89], activating RAGE-mediated signaling pathways. Mondola P et al [90] demonstrated that SOD1 induces Ca^{2+} increase through intracellular and extracellular-dependent mechanisms and that SOD1, in addition to acting as a scavenger of superoxide radicals, can also induce Ca^{2+} increase through intracellular and extracellular-dependent mechanisms, further affecting different biological functions. S100A13, as a Ca^{2+} binding protein, is bound to be somewhat affected by SOD1-induced changes in Ca^{2+} content.

PPP2R2A is one of the regulatory subunits of PP2A, and Akt is one of the substrates of PP2A, which is closely related to the development of DM and its complications. PPP2R2A inhibits the Akt pathway by inducing p-Akt dephosphorylation [91] and thus inactivating Akt function. Our data clearly show that PPP2R2A expression activity was upregulated in the DN group compared to the NC group, at which point it was a protective upregulation response due to oxidative stress, while the DN-DAPA group showed downregulation of this protein expression compared to the DN group, suggesting that the application of dapagliflozin may inhibit PPP2R2A activity and thus play a role in the repair of early DN damage.

From the results of GO enrichment analysis, we found that the Cellular Component of differential proteins gradually changed from extracellular space to nuclear lumen, nucleoplasm, and mitochondria-associated protein complexes under the effect of dapagliflozin, and we can confidently speculate that the mechanism of dapagliflozin action is through the action of Mitochondria, and the application of dapagliflozin has led to more differential proteins with phosphatase function in Molecular function, phosphorylation is pivotal for glucose metabolism and energy storage and release, and also plays a key role in signaling pathways [92]. In summary, dapagliflozin acts mainly in mitochondria, conferring differential protein phosphorylation. It may regulate mitochondrial dysfunction and oxidative stress injury, attenuate early renal lesions, and suppress microalbuminuria by engaging in ROS-dependent inhibition of PPP2R2A and CXCL12/S100A13 pathways. Therefore, this signaling pathway may be a target for clinical treatment of DN, and dapagliflozin acts through this pathway, and the specific mechanism needs to be further investigated.

5. Conclusion

Dapagliflozin improves early DN and reduces the severity of microproteinuria by downregulating PPP2R2A and CXCL12/S100A13 through a ROS-dependent mechanism. The present work only provides a proof-of-concept framework for the improvement mechanism of dapagliflozin in mild to moderate DN microproteinuria, and further studies are necessary. There is no denying that our study has some flaws. Firstly, the above predictions were not confirmed experimentally and the study of the mechanism of dapagliflozin action in microproteinuria is relatively preliminary; secondly, the sample size of this study is relatively small.

Declarations

-Ethics approval and consent to participate

The experimental protocol was established, according to the ethical guidelines of the Helsinki Declaration and was approved by the Human Ethics Committee of Ethics Committee of the Second Hospital of Jilin University. Consent was obtained from individual participants. Informed consent was obtained from individual participants. All methods were performed in accordance with the relevant and recognized guidelines and regulations.

-Consent for publication

Not applicable

-Availability of data and materials

All data generated during this study are included in this published article

-Competing interests

The authors state that they have no conflicting interests.

-Funding

This study was supported by Jilin Province Health and health technology innovation project 2020J040 .

-Authors' contributions

Author's roles: Designed research: Cai Hanqing Yang Maoguang; Performed research: Wang Suhong, Ning Lili; Analyzed data: Wang Suhong, Cheng Yan; Wrote the manuscript: Wang Suhong, Yang Maoguang; Revised the manuscript: Wang Suhong, Yang Maoguang, Cheng Yan, Ning Lili, Li Mo, Yan Yan, Shen Hong, Cai Hanqing; All authors approved the final version of the manuscript. Wang Suhong, Yang Maoguang take responsibility for the integrity of the data analysis.

-Acknowledgements

The authors wish to thank all the participants for completing the study. We would like to also thank the Jilin Province Health and health technology innovation project for funding this study.

References

1. Williams R, Karuranga S, Malanda B, et al., *Global and regional estimates and projections of diabetes-related health expenditure: Results from the International Diabetes Federation Diabetes Atlas, 9th edition*. Diabetes Research and Clinical Practice, 2020. **162**.
2. Li K X, Ji M J, and Sun H J, *An updated pharmacological insight of resveratrol in the treatment of diabetic nephropathy*. Gene, 2021. **780**: p. 145532.
3. Conserva F, Barozzino M, Pesce F, et al., *Urinary miRNA-27b-3p and miRNA-1228-3p correlate with the progression of Kidney Fibrosis in Diabetic Nephropathy*. Scientific Reports, 2019. **9**.
4. Gruden G, Perin P C, and Camussi G, *Insight on the pathogenesis of diabetic nephropathy from the study of podocyte and mesangial cell biology*. Curr Diabetes Rev, 2005. **1**(1): p. 27–40.
5. Mogensen C E, Schmitz A, and Christensen C K, *Comparative renal pathophysiology relevant to IDDM and NIDDM patients*. Diabetes Metab Rev, 1988. **4**(5): p. 453–83.
6. Rajasekeran H, Cherney D Z, and Lovshin J A, *Do effects of sodium-glucose cotransporter-2 inhibitors in patients with diabetes give insight into potential use in non-diabetic kidney disease?* Current Opinion in Nephrology and Hypertension, 2017. **26**(5): p. 358–367.
7. DeFronzo R A, Norton L, and Abdul-Ghani M, *Renal, metabolic and cardiovascular considerations of SGLT2 inhibition*. Nature Reviews Nephrology, 2017. **13**(1): p. 11–26.
8. Li C, Zhang J, Xue M, et al., *SGLT2 inhibition with empagliflozin attenuates myocardial oxidative stress and fibrosis in diabetic mice heart*. Cardiovasc Diabetol, 2019. **18**(1): p. 15.
9. Merovci A, Solis-Herrera C, Daniele G, et al., *Dapagliflozin improves muscle insulin sensitivity but enhances endogenous glucose production*. Journal of Clinical Investigation, 2014. **124**(2): p. 509–514.
10. Wang X X X, Levi J, Luo Y H, et al., *SGLT2 Protein Expression Is Increased in Human Diabetic Nephropathy SGLT2 PROTEIN INHIBITION DECREASES RENAL LIPID ACCUMULATION*,

- INFLAMMATION, AND THE DEVELOPMENT OF NEPHROPATHY IN DIABETIC MICE*. Journal of Biological Chemistry, 2017. **292**(13): p. 5335–5348.
11. Fioretto P, Zambon A, Rossato M, et al., *SGLT2 Inhibitors and the Diabetic Kidney*. Diabetes Care, 2016. **39**: p. S165-S171.
 12. Perkovic V, Jardine M J, Neal B, et al., *Canagliflozin and Renal Outcomes in Type 2 Diabetes and Nephropathy*. New England Journal of Medicine, 2019. **380**(24): p. 2295–2306.
 13. Wanner C, *EMPA-REG OUTCOME: The Nephrologist's Point of View*. American Journal of Cardiology, 2017. **120**(1): p. S59-S67.
 14. Wiviott S D, Raz I, Bonaca M P, et al., *Dapagliflozin and Cardiovascular Outcomes in Type 2 Diabetes*. New England Journal of Medicine, 2019. **380**(4): p. 347–357.
 15. Dihazi H, *Clinical proteomics: an insight into the urinary proteome*. Expert Review of Proteomics, 2006. **3**(5): p. 481–482.
 16. Knepper M A, *Proteomics and the kidney*. J Am Soc Nephrol, 2002. **13**(5): p. 1398–408.
 17. Ashburner M, Ball C A, Blake J A, et al., *Gene ontology: tool for the unification of biology. The Gene Ontology Consortium*. Nat Genet, 2000. **25**(1): p. 25–9.
 18. Kanehisa M and Goto S, *KEGG: kyoto encyclopedia of genes and genomes*. Nucleic Acids Res, 2000. **28**(1): p. 27–30.
 19. Bandeira S D, da Fonseca L J S, Guedes G D, et al., *Oxidative Stress as an Underlying Contributor in the Development of Chronic Complications in Diabetes Mellitus*. International Journal of Molecular Sciences, 2013. **14**(2): p. 3265–3284.
 20. Kumar P, Raman T, Swain M M, et al., *Hyperglycemia-Induced Oxidative-Nitrosative Stress Induces Inflammation and Neurodegeneration via Augmented Tuberous Sclerosis Complex-2 (TSC-2) Activation in Neuronal Cells*. Molecular Neurobiology, 2017. **54**(1): p. 238–254.
 21. Brennan R, Docherty N G, Neff K J, et al., *Comparing the Effect of Roux-En-Y Gastric Bypass on Proteinuria and Renal Inflammation in a Rat Model of Type 2 Diabetes and Diabetic Kidney Disease*. Irish Journal of Medical Science, 2014. **183**: p. S547-S547.
 22. Elmarakby A A and Sullivan J C, *Relationship between Oxidative Stress and Inflammatory Cytokines in Diabetic Nephropathy*. Cardiovascular Therapeutics, 2012. **30**(1): p. 49–59.
 23. Duni A, Liakopoulos V, Roumeliotis S, et al., *Oxidative Stress in the Pathogenesis and Evolution of Chronic Kidney Disease: Untangling Ariadne's Thread*. International Journal of Molecular Sciences, 2019. **20**(15).
 24. Wang X, Huang R, Zhang L, et al., *A severe atherosclerosis mouse model on the resistant NOD background*. Dis Model Mech, 2018. **11**(10).
 25. Schieber M and Chandel N S, *ROS Function in Redox Signaling and Oxidative Stress*. Current Biology, 2014. **24**(10): p. R453-R462.
 26. Hekimi S, Lapointe J, and Wen Y, *Taking a "good" look at free radicals in the aging process*. Trends in Cell Biology, 2011. **21**(10): p. 569–576.

27. Xie M and Roy R, *Increased Levels of Hydrogen Peroxide Induce a HIF-1-dependent Modification of Lipid Metabolism in AMPK Compromised C. elegans Dauer Larvae*. Cell Metabolism, 2012. **16**(3): p. 322–335.
28. Sahajpal N S, Goel R K, Chaubey A, et al., *Pathological Perturbations in Diabetic Retinopathy: Hyperglycemia, AGEs, Oxidative Stress and Inflammatory Pathways*. Current Protein & Peptide Science, 2019. **20**(1): p. 92–110.
29. Rosen P, Nawroth P P, King G, et al., *The role of oxidative stress in the onset and progression of diabetes and its complications: a summary of a Congress Series sponsored by UNESCO-MCBN, the American Diabetes Association and the German Diabetes Society*. Diabetes Metab Res Rev, 2001. **17**(3): p. 189–212.
30. Coughlan M T, Mibus A L, and Forbes J M, *Oxidative stress and advanced glycation in diabetic nephropathy*. Ann N Y Acad Sci, 2008. **1126**: p. 190–3.
31. Kumar P, Rao G N, Pal B B, et al., *Hyperglycemia-induced oxidative stress induces apoptosis by inhibiting PI3-kinase/Akt and ERK1/2 MAPK mediated signaling pathway causing downregulation of 8-oxoG-DNA glycosylase levels in glial cells*. Int J Biochem Cell Biol, 2014. **53**: p. 302–19.
32. Widlansky M E, Wang J, Shenouda S M, et al., *Altered mitochondrial membrane potential, mass, and morphology in the mononuclear cells of humans with type 2 diabetes*. Transl Res, 2010. **156**(1): p. 15–25.
33. Forbes J M, Coughlan M T, and Cooper M E, *Oxidative stress as a major culprit in kidney disease in diabetes*. Diabetes, 2008. **57**(6): p. 1446–1454.
34. Brownlee M, *The pathobiology of diabetic complications - A unifying mechanism*. Diabetes, 2005. **54**(6): p. 1615–1625.
35. Forbes J M and Cooper M E, *Mechanisms of diabetic complications*. Physiol Rev, 2013. **93**(1): p. 137–88.
36. Bhatt M P, Lim Y C, Hwang J, et al., *C-Peptide Prevents Hyperglycemia-Induced Endothelial Apoptosis Through Inhibition of Reactive Oxygen Species-Mediated Transglutaminase 2 Activation*. Diabetes, 2013. **62**(1): p. 243–253.
37. Uruno A, Furusawa Y, Yagishita Y, et al., *The Keap1-Nrf2 System Prevents Onset of Diabetes Mellitus*. Molecular and Cellular Biology, 2013. **33**(15): p. 2996–3010.
38. Kim J, Kim C S, Kim H, et al., *Protection against advanced glycation end products and oxidative stress during the development of diabetic keratopathy by KIOM-79*. Journal of Pharmacy and Pharmacology, 2011. **63**(4): p. 524–530.
39. Lal M A, Brismar H, Eklof A C, et al., *Role of oxidative stress in advanced glycation end product-induced mesangial cell activation*. Kidney Int, 2002. **61**(6): p. 2006–14.
40. Tervaert T W C, Mooyaart A L, Amann K, et al., *Pathologic Classification of Diabetic Nephropathy*. Journal of the American Society of Nephrology, 2010. **21**(4): p. 556–563.
41. Giacco F and Brownlee M, *Oxidative Stress and Diabetic Complications*. Circulation Research, 2010. **107**(9): p. 1058–1070.

42. Coughlan M T, Nguyen T V, Penfold S A, et al., *Mapping time-course mitochondrial adaptations in the kidney in experimental diabetes*. *Clinical Science*, 2016. **130**(9): p. 711–720.
43. Tan A L Y, Sourris K C, Harcourt B E, et al., *Disparate effects on renal and oxidative parameters following RAGE deletion, AGE accumulation inhibition, or dietary AGE control in experimental diabetic nephropathy*. *American Journal of Physiology-Renal Physiology*, 2010. **298**(3): p. F763-F770.
44. Dugan L L, You Y H, Ali S S, et al., *AMPK dysregulation promotes diabetes-related reduction of superoxide and mitochondrial function*. *Journal of Clinical Investigation*, 2013. **123**(11): p. 4888–4899.
45. Cogliati S, Frezza C, Soriano M E, et al., *Mitochondrial Cristae Shape Determines Respiratory Chain Supercomplexes Assembly and Respiratory Efficiency*. *Cell*, 2013. **155**(1): p. 160–171.
46. Bhargava P and Schnellmann R G, *Mitochondrial energetics in the kidney*. *Nature Reviews Nephrology*, 2017. **13**(10): p. 629–646.
47. Reidy K, Kang H M, Hostetter T, et al., *Molecular mechanisms of diabetic kidney disease*. *J Clin Invest*, 2014. **124**(6): p. 2333–40.
48. Reddy M A and Natarajan R, *Epigenetics in diabetic kidney disease*. *J Am Soc Nephrol*, 2011. **22**(12): p. 2182–5.
49. Kalyanaraman B, *Teaching the basics of cancer metabolism: Developing antitumor strategies by exploiting the differences between normal and cancer cell metabolism*. *Redox Biology*, 2017. **12**: p. 833–842.
50. Zhang Y F, Feng J X, Wang Q, et al., *Hyperglycaemia Stress-Induced Renal Injury is Caused by Extensive Mitochondrial Fragmentation, Attenuated MKP1 Signalling, and Activated JNK-CaMKII-Fis1 Biological Axis*. *Cellular Physiology and Biochemistry*, 2018. **51**(4): p. 1778–1798.
51. Durak A, Olgar Y, Degirmenci S, et al., *A SGLT2 inhibitor dapagliflozin suppresses prolonged ventricular-repolarization through augmentation of mitochondrial function in insulin-resistant metabolic syndrome rats*. *Cardiovascular Diabetology*, 2018. **17**.
52. Tanajak P, Sa-nguanmoo P, Sivasinprasasn S, et al., *Cardioprotection of dapagliflozin and vildagliptin in rats with cardiac ischemia-reperfusion injury*. *Journal of Endocrinology*, 2018. **236**(2): p. 69–84.
53. Maejima Y, *SGLT2 Inhibitors Play a Salutary Role in Heart Failure via Modulation of the Mitochondrial Function*. *Frontiers in Cardiovascular Medicine*, 2020. **6**.
54. Taniguchi N, *Clinical significances of superoxide dismutases: changes in aging, diabetes, ischemia, and cancer*. *Adv Clin Chem*, 1992. **29**: p. 1–59.
55. Fujita H, Fujishima H, Chida S, et al., *Reduction of Renal Superoxide Dismutase in Progressive Diabetic Nephropathy*. *Journal of the American Society of Nephrology*, 2009. **20**(6): p. 1303–1313.
56. Offer T, Russo A, and Samuni A, *The pro-oxidative activity of SOD and nitroxide SOD mimics*. *Faseb Journal*, 2000. **14**(9): p. 1215–1223.
57. Okado-Matsumoto A and Fridovich I, *Subcellular distribution of superoxide dismutases (SOD) in rat liver: Cu,Zn-SOD in mitochondria*. *J Biol Chem*, 2001. **276**(42): p. 38388–93.

58. Rojo A I, Salinas M, Martin D, et al., *Regulation of Cu/Zn-superoxide dismutase expression via the phosphatidylinositol 3 kinase/Akt pathway and nuclear factor-kappaB*. J Neurosci, 2004. **24**(33): p. 7324–34.
59. Gong D, Chen X, Middleditch M, et al., *Quantitative proteomic profiling identifies new renal targets of copper(II)-selective chelation in the reversal of diabetic nephropathy in rats*. Proteomics, 2009. **9**(18): p. 4309–20.
60. Zhang M, Zhang J Z, Xiong Y, et al., *Pyroloquinoline Quinone Inhibits Oxidative Stress in Rats with Diabetic Nephropathy*. Medical Science Monitor, 2020. **26**.
61. Bhatia S, Shukla R, Venkata Madhu S, et al., *Antioxidant status, lipid peroxidation and nitric oxide end products in patients of type 2 diabetes mellitus with nephropathy*. Clin Biochem, 2003. **36**(7): p. 557–62.
62. DeRubertis F R, Craven P A, and Melhem M F, *Acceleration of diabetic renal injury in the superoxide dismutase knockout mouse: effects of tempol*. Metabolism-Clinical and Experimental, 2007. **56**(9): p. 1256–1264.
63. Rodrigues A M, Serralha R S, Lima D Y, et al., *P2X7 siRNA targeted to the kidneys increases klotho and delays the progression of experimental diabetic nephropathy*. Purinergic Signalling, 2020. **16**(2): p. 175–185.
64. Craven P A, Melhem M F, Phillips S L, et al., *Overexpression of Cu²⁺/Zn²⁺ + superoxide dismutase protects against early diabetic glomerular injury in transgenic mice*. Diabetes, 2001. **50**(9): p. 2114–2125.
65. DeRubertis F R, Craven P A, Melhem M F, et al., *Attenuation of renal injury in db/db mice overexpressing superoxide dismutase - Evidence for reduced superoxide-nitric oxide interaction*. Diabetes, 2004. **53**(3): p. 762–768.
66. Kim S M, Lee S H, Kim Y G, et al., *Hyperuricemia-induced NLRP3 activation of macrophages contributes to the progression of diabetic nephropathy*. Am J Physiol Renal Physiol, 2015. **308**(9): p. F993-F1003.
67. Zhang Y Y, Depond M, He L, et al., *CXCR4/CXCL12 axis counteracts hematopoietic stem cell exhaustion through selective protection against oxidative stress*. Scientific Reports, 2016. **6**.
68. Yu L, Cecil J, Peng S B, et al., *Identification and expression of novel isoforms of human stromal cell-derived factor 1*. Gene, 2006. **374**: p. 174–9.
69. Janssens R, Struyf S, and Proost P, *The unique structural and functional features of CXCL12*. Cell Mol Immunol, 2018. **15**(4): p. 299–311.
70. Yano T, Liu Z Y, Donovan J, et al., *Stromal cell-derived factor-1 (SDF-1)/CXCL12 attenuates diabetes in mice and promotes pancreatic beta-cell survival by activation of the prosurvival kinase Akt*. Diabetes, 2007. **56**(12): p. 2946–2957.
71. Stokman G, Stroo I, Claessen N, et al., *SDF-1 provides morphological and functional protection against renal ischaemia/reperfusion injury*. Nephrology Dialysis Transplantation, 2010. **25**(12): p. 3852–3859.

72. Yu B B, Zhi H, Zhang X Y, et al., *Mitochondrial dysfunction-mediated decline in angiogenic capacity of endothelial progenitor cells is associated with capillary rarefaction in patients with hypertension via downregulation of CXCR4/JAK2/SIRT5 signaling*. *Ebiomedicine*, 2019. **42**: p. 64–75.
73. Liu R J, Zhong Y F, Li X Z, et al., *Role of Transcription Factor Acetylation in Diabetic Kidney Disease*. *Diabetes*, 2014. **63**(7): p. 2440–2453.
74. Young B, Purcell C, Kuang Y Q, et al., *Superoxide Dismutase 1 Regulation of CXCR4-Mediated Signaling in Prostate Cancer Cells is Dependent on Cellular Oxidative State*. *Cellular Physiology and Biochemistry*, 2015. **37**(6): p. 2071–2084.
75. Feliers D, Chen X Y, Akis N, et al., *VEGF regulation of endothelial nitric oxide synthase in glomerular endothelial cells*. *Kidney International*, 2005. **68**(4): p. 1648–1659.
76. Sun Y, Deng M, Ke X, et al., *Epidermal Growth Factor Protects Against High Glucose-Induced Podocyte Injury Possibly via Modulation of Autophagy and PI3K/AKT/mTOR Signaling Pathway Through DNA Methylation*. *Diabetes Metabolic Syndrome and Obesity-Targets and Therapy*, 2021. **14**: p. 2255–2268.
77. Humes H D, Cieslinski D A, Coimbra T M, et al., *Epidermal growth factor enhances renal tubule cell regeneration and repair and accelerates the recovery of renal function in postischemic acute renal failure*. *J Clin Invest*, 1989. **84**(6): p. 1757–61.
78. Coimbra T M, Cieslinski D A, and Humes H D, *Epidermal growth factor accelerates renal repair in mercuric chloride nephrotoxicity*. *Am J Physiol*, 1990. **259**(3 Pt 2): p. F438-43.
79. Stepien G, Torroni A, Chung A B, et al., *Differential expression of adenine nucleotide translocator isoforms in mammalian tissues and during muscle cell differentiation*. *J Biol Chem*, 1992. **267**(21): p. 14592–7.
80. Clemencon B, Babot M, and Trezeguet V, *The mitochondrial ADP/ATP carrier (SLC25 family): Pathological implications of its dysfunction*. *Molecular Aspects of Medicine*, 2013. **34**(2–3): p. 485–493.
81. De Giorgi F, Lartigue L, Bauer M K, et al., *The permeability transition pore signals apoptosis by directing Bax translocation and multimerization*. *FASEB J*, 2002. **16**(6): p. 607–9.
82. Zhu P J, Hu S Y, Jin Q H, et al., *Ripk3 promotes ER stress-induced necroptosis in cardiac IR injury: A mechanism involving calcium overload/XO/ROS/mPTP pathway*. *Redox Biology*, 2018. **16**: p. 157–168.
83. Inoue O, Hokamura K, Shirai T, et al., *Vascular Smooth Muscle Cells Stimulate Platelets and Facilitate Thrombus Formation through Platelet CLEC-2: Implications in Atherothrombosis*. *Plos One*, 2015. **10**(9).
84. Lambros M P, Parsa C, Mulamalla H, et al., *Identifying cell and molecular stress after radiation in a three-dimensional (3-D) model of oral mucositis*. *Biochemical and Biophysical Research Communications*, 2011. **405**(1): p. 102–106.
85. Hofmann M A, Drury S, Fu C, et al., *RAGE mediates a novel proinflammatory axis: a central cell surface receptor for S100/calgranulin polypeptides*. *Cell*, 1999. **97**(7): p. 889–901.

86. Chazin W J, *Relating form and function of EF-hand calcium binding proteins*. Acc Chem Res, 2011. **44**(3): p. 171–9.
87. Orlova V V, Choi E Y, Xie C P, et al., *A novel pathway of HMGB1-mediated inflammatory cell recruitment that requires Mac-1-integrin*. Embo Journal, 2007. **26**(4): p. 1129–1139.
88. Schmidt A M, Hofmann M, Taguchi A, et al., *RAGE: A multiligand receptor contributing to the cellular response in diabetic vasculopathy and inflammation*. Seminars in Thrombosis and Hemostasis, 2000. **26**(5): p. 485–493.
89. Donato R, *RAGE: A single receptor for several ligands and different cellular responses: The case of certain S100 proteins*. Current Molecular Medicine, 2007. **7**(8): p. 711–724.
90. Mondola P, Damiano S, Sasso A, et al., *The Cu, Zn Superoxide Dismutase: Not Only a Dismutase Enzyme*. Front Physiol, 2016. **7**: p. 594.
91. Zhang Y Z, Ma T, Yang S P, et al., *High-mobility group A1 proteins enhance the expression of the oncogenic miR-222 in lung cancer cells*. Molecular and Cellular Biochemistry, 2011. **357**(1–2): p. 363–371.
92. Kresge N, Simoni R D, and Hill R L, *The process of reversible phosphorylation: the work of Edmond H. Fischer*. J Biol Chem, 2011. **286**(3): p. e1-2.

Tables

Table 1 Inclusion and exclusion criteria for this study

Inclusion and exclusion criteria

Inclusion criteria

- Male or female with age ≥ 40 years and < 75 years
- Diagnosed with type 2 DM (WHO criteria in 1999)^[18]
- DN standard refers to Mogensen staging I~III stages
- The urinary microalbumin/creatinine ratio was ≥ 30 mg/g Cr in 2 out of 3 times detected within 3 months eGFR ≥ 60 ml/min/1.73m²
- Patients with DR
- Body mass index between 18.5-30 kg/m²
- The patient must be willing and able to comply with the protocol for the duration of the study
- Eligible patients had chronic kidney disease secondary to T2DM eGFR reduce (30-60 mL/min/1.73 m²) Or UACR between 30-300 mg/g

Exclusion criteria

- Average of systolic BP > 150 mm Hg at calm
- Average of diastolic BP > 90 mm Hg at calm
- Type 1 DM (WHO criteria in 1999)
- Current in treatment with more than one RAAS blocking agent
- Gestational diabetes and special type diabetes
- DKA or HHS or other acute complications of diabetes
- Primary glomerular disease
- Hypertensive nephropathy
- Renal arteriosclerosis
- Other autoimmune diseases which lead to Kidney damage
- Drug induced renal damage
- Acute renal insufficiency, infection, trauma, surgery, severe cardiovascular and cerebrovascular diseases, tumors, other systemic diseases and stress, failure to comply with the program
- Renal stone, renal cyst, renal effusion, urinary tract infection and other factors that affect renal function and urinary protein

DR Diabetic retinopathy eGFR Estimate glomerular filtration rate BMI body mass index UACR Urine albumin creatine ratio BP blood pressure T1DM Type 1 diabetes mellitus RASS Renin-angiotensin-aldosterone system DKA Diabetic ketoacidosis HHS Hyperosmolar hyperglycemia syndrome

Table 2. Table of baseline information

	Unit	DN [n=5]	DN-DAPA (n=5)	NC (n=5)	p-value
Sex	Male/Female	3/2		2/3	0.765
Age	years	61±4.74		51±8.39	1.00
Course of the disease	years	7(3.00 22.50)		-	-
BMI	kg/cm ²	27.10±2.00	26.45±3.00	21.78±0.75	0.698
HbA1c	%	8.52±0.59	7.12±0.89	5.22±0.41	0.019
FPG	mmol/L	8.70±2.33	6.85±0.93	5.46±0.36	0.158
Scr	mg/dl	64.60±16.11	62.80±16.08	57.40±10.53	0.864
UA	mmol/L	345.80±105.33	293.0±61.11	358.20±84.11	0.361
SBP	mmHg	139.00±5.48	139.60±7.13	122.60±10.07	0.885
DBP	mmHg	90(80,95)	90(87.50,92.50)	85(75,90)	0.323
TC	mmol/L	4.10±0.82	4.66±0.94	4.59±0.46	0.338
TG	mmol/L	2.09±1.86	2.95±2.57	2.45±0.89	0.563
LDL	mmol/L	2.48±1.06	2.73±1.08	2.72±0.48	0.714
eGFR	60ml/min/ 1.73m ²	100.8(90.10,103.25)	103.1(87.25,105.7)	105.2(100.85,107.1)	0.331

Table 3. Differential proteins and differential expression ploidy described in this paper

Gene name	DN/NC			DN-DAPA/DN		
	Regulated Type	Ratio	P-value	Regulated Type	Ratio	P-value
SOD1	Up	10.0041	0.0043	Down	5.4645	0.0139
SLC25A6	Up	3.8356	0.0382	Down	4.0080	0.0200
PPP2R2A	Up	2.3420	0.0067	Down	2.9317	0.0490
S100A13	Up	2.1409	0.0063	Down	1.9026	0.0392
CXCL12	Up	1.6263	0.0395	Down	1.8291	0.0053

CXCL12 Stromal cell-derived factor 1 SOD1 Superoxide dismutase[Cu-Zn] S100A13 Protein S100-A13
 PPP2R2A Serine/threonine-protein phosphatase 2A55 kDa regulatory subunit B alpha isoform SLC25A6
 ADP/ATP translocase 3

Figures

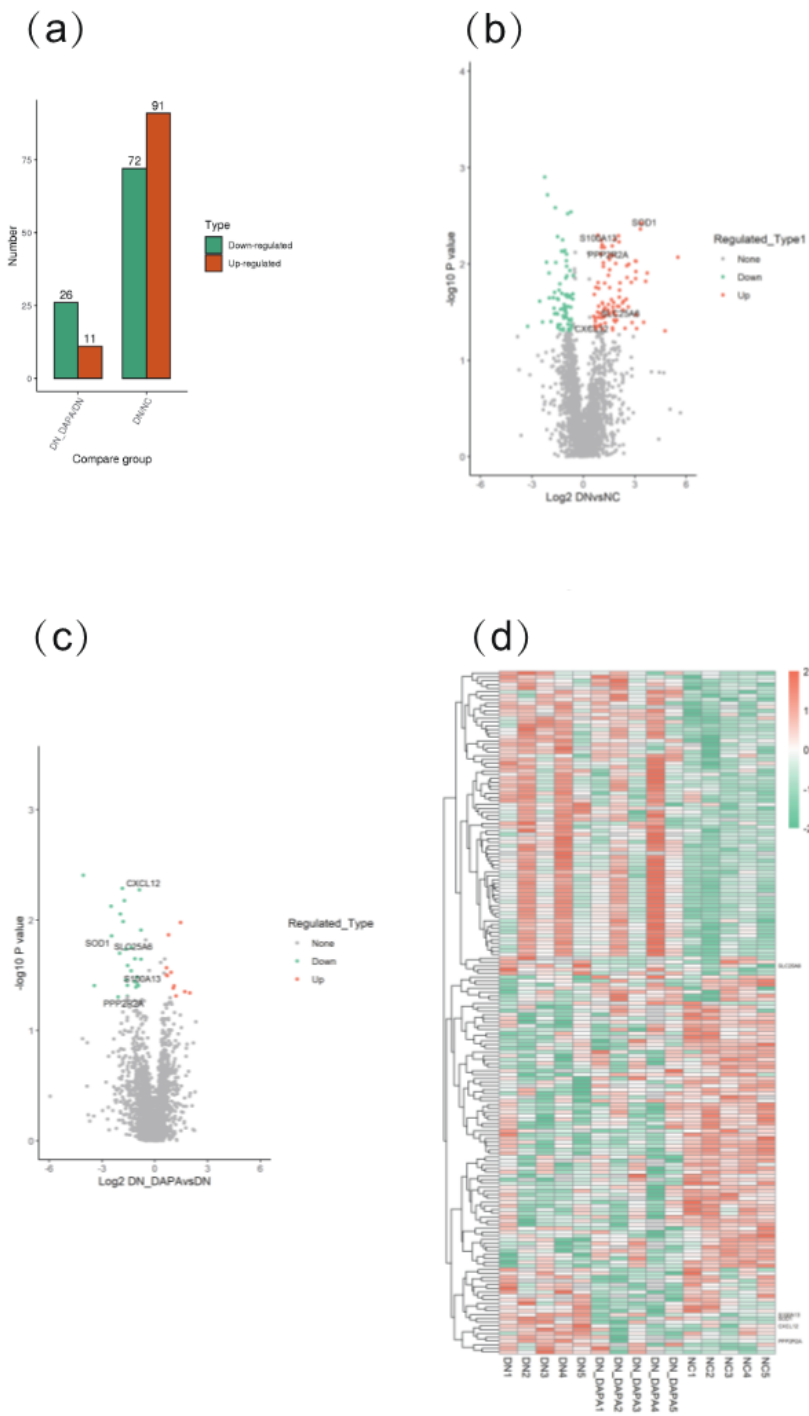


Figure 1

Differential protein volcano map and heat map of DN/NC group and DN-DAPA/DN group

A: Differentially expressed protein data. Green represents the number of proteins expressed down-regulated in both groups: 26 expressed down-regulated proteins in the DN-DAPA/DN group and 72 expressed down-regulated proteins in the DN/NC group; red represents the number of proteins expressed up-regulated in both groups: 11 expressed up-regulated proteins in the DN-DAPA/DN group and 91 expressed up-regulated

proteins in the DN/NC group. b: DN/NC group Volcano plot analysis identified differential proteins, red dots represent protein up-regulation and green dots represent protein down-regulation. c: volcano plot analysis of DN-DAPA/DN group identified differential proteins, red dots represent protein up-regulation and green dots represent protein down-regulation. d: heat map showing red region for highly expressed proteins and green region for lowly expressed proteins.

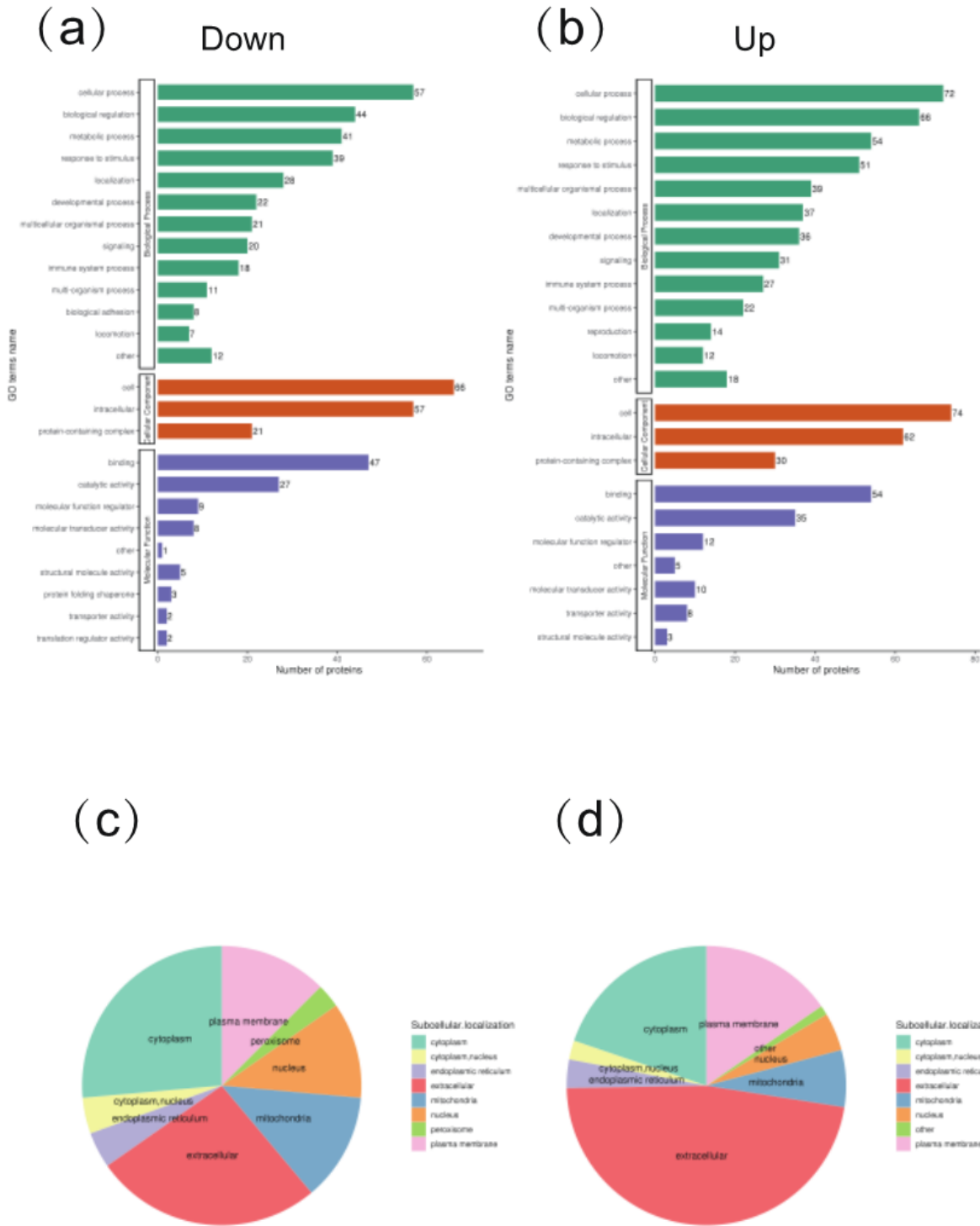
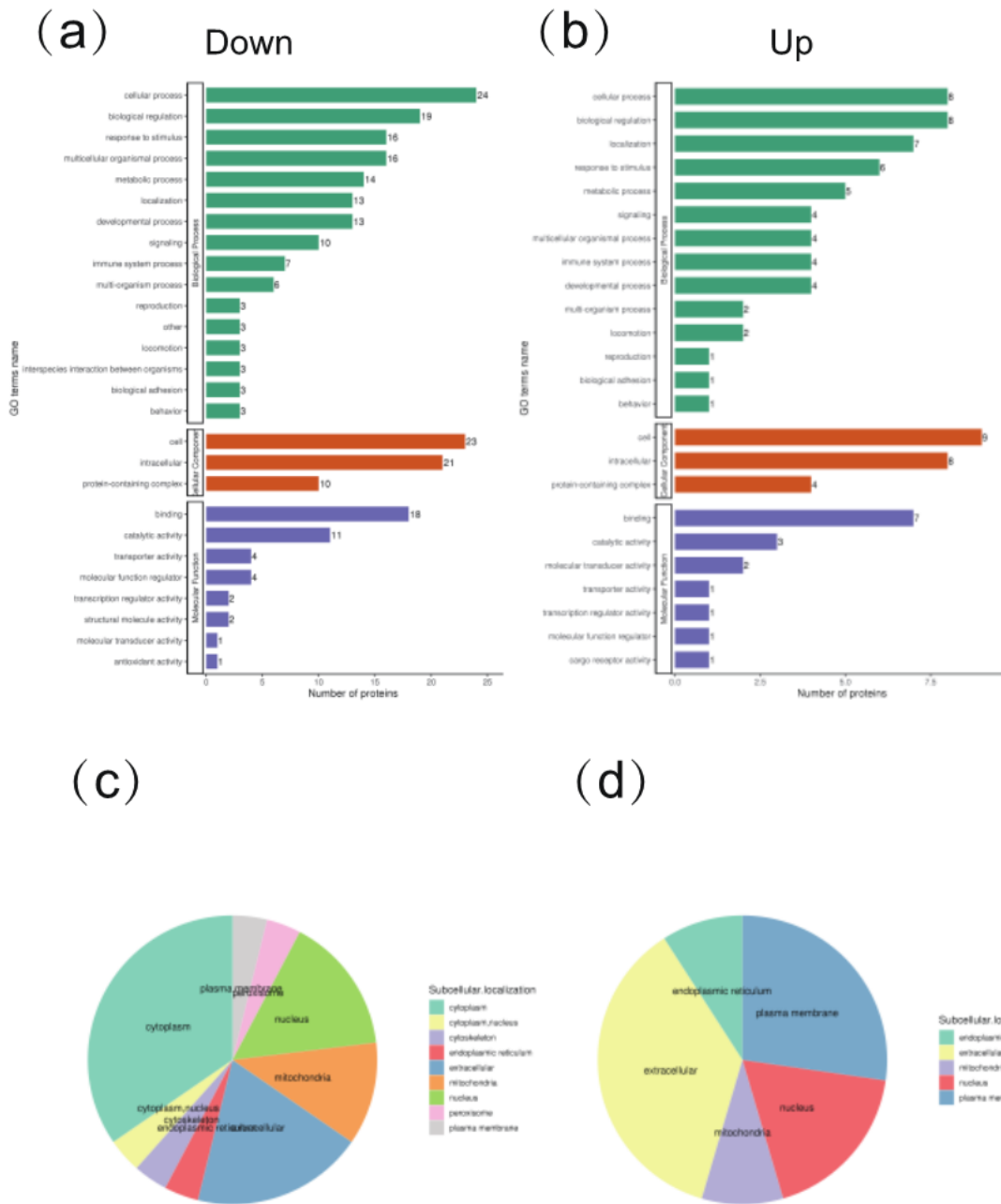


Figure 2

Classification of GO secondary annotation and subcellular structure annotation of DN/NC group.

A: GO secondary classification involving differentially expressed down-regulated proteins. B: GO secondary classification involving differentially expressed up-regulated proteins. C: Subcellular localization of differentially expressed down-regulated proteins. D: Subcellular localization of differentially expressed up-regulated proteins.

The subcellular structural localization of the down-regulated proteins in the DN/NC group, in descending order of protein number, were: cytoplasm, extracellular, cell membrane, mitochondria, nucleus, cytoplasm, nucleus, endoplasmic reticulum, peroxisome (Figure 2C); the up-regulated proteins were located in descending order of protein number: extracellular, cytoplasm, cytoplasmic membrane, mitochondria, endoplasmic reticulum, cytoplasm, nucleus, others (Figure 2D).



DN_DAPA/DN

Figure 3

Classification of GO secondary annotation and subcellular structure annotation of DN-DAPA/DN group.

A: GO secondary classification involving differentially expressed down-regulated proteins. B: GO secondary classification involving differentially expressed up-regulated proteins. C: Subcellular localization of differentially expressed down-regulated proteins. D: Subcellular localization of differentially expressed up-regulated proteins.

The subcellular structural localization of the down-regulated proteins in the DN/NC group, in descending order of protein number, were: cytoplasm, extracellular, nucleus, mitochondria, cytoplasm, nucleus, cytoskeleton, endoplasmic reticulum, peroxisome, and cytoplasmic membrane (Figure 3C); the up-regulated proteins were located in descending order of protein number: extracellular, cytoplasmic membrane, nucleus, endoplasmic reticulum, and mitochondria (Figure 3D).

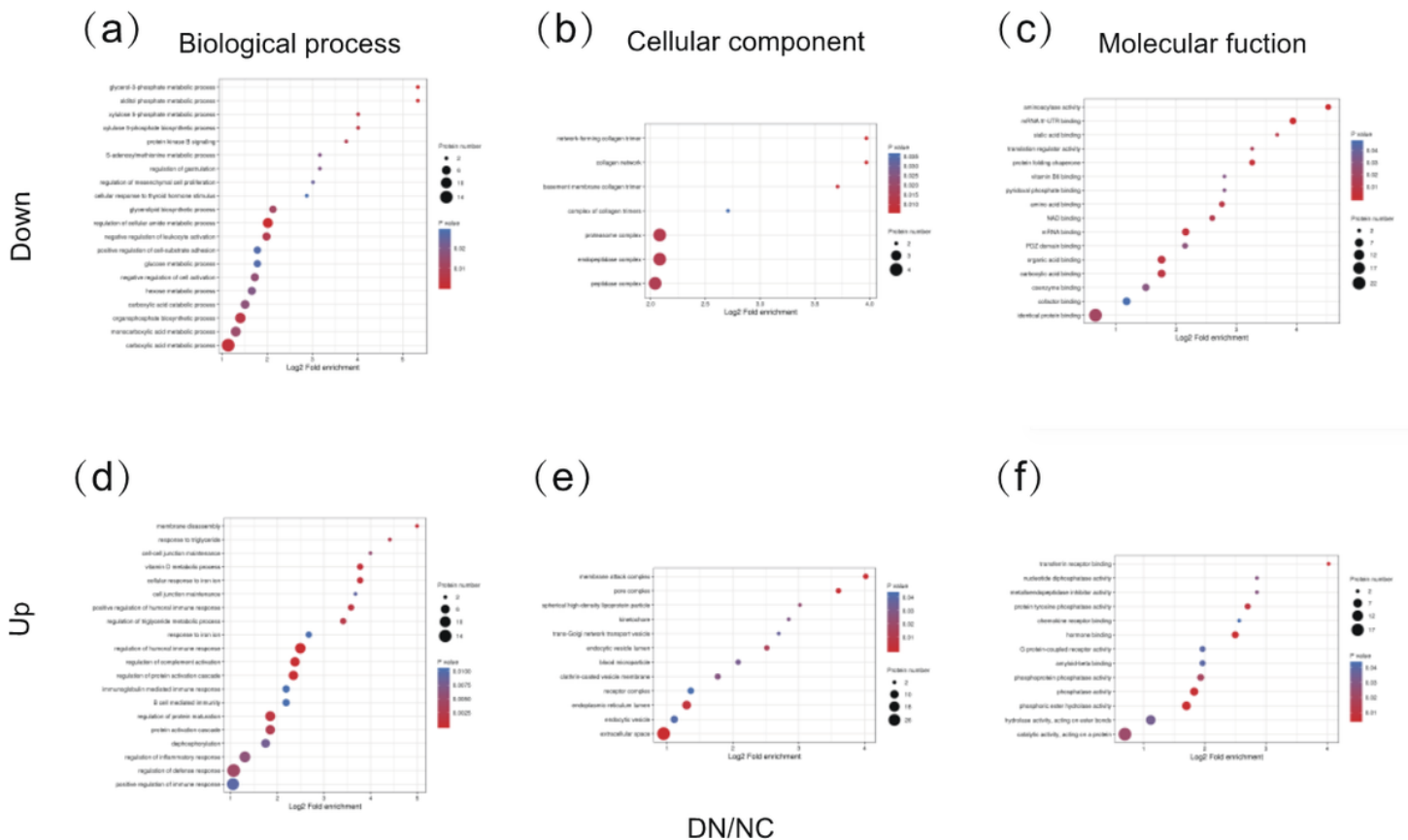


Figure 4

GO enrichment analysis of differentially expressed proteins in DN/NC group

A: down-regulated protein involved in BP. B: a down-regulated protein involved in CC. C: a down-regulated protein involved in MF. D: an up-regulated protein involved in BP.

All upregulated differential protein BP analysis involved important pathways such as regulation of humoral immune response, regulation of complement activation, and regulation of protein activation cascade (Figure 4D). cc mainly showed in extracellular space, membrane attack complex, pore complex (Figure 4E). classification of MF showed hormone binding, phosphoric ester hydrolase activity, transferrin receptor binding (Figure 4F).

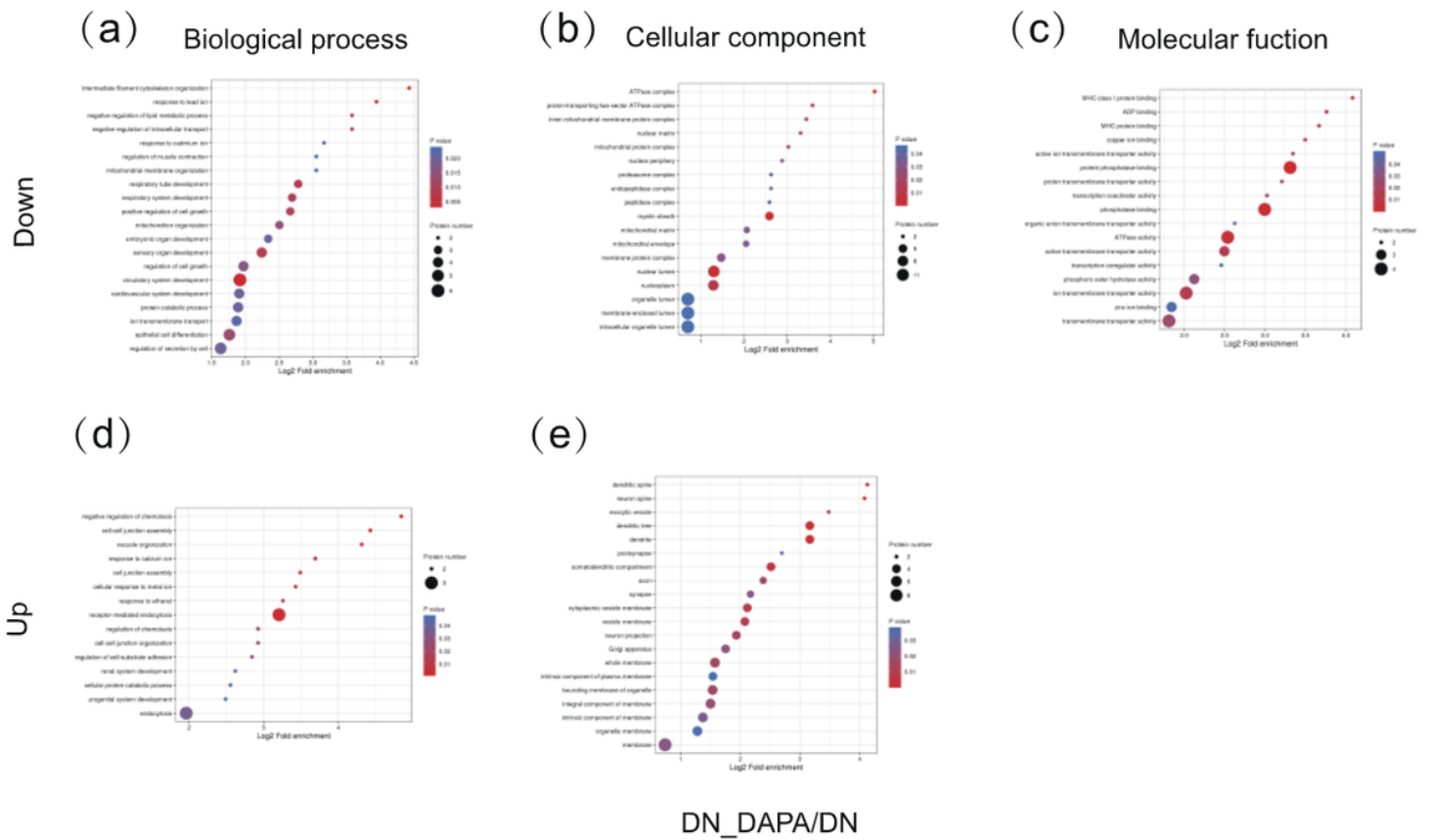


Figure 5

GO enrichment analysis of differentially expressed proteins in DN-DAPA/DN group

A: down-regulated protein involved in BP. B: a down-regulated protein involved in CC. C: a down-regulated protein involved in MF. D: an up-regulated protein involved in BP.

In DN-DAPA/DN, all down-regulated differential proteins with the highest BP enrichment were the terms intermediate filament cytoskeleton organization, circulatory system development, and response to lead ion (Figure 5A). CC was myelin sheath, ATPase complex, nuclear lumen (Figure 5B). MF was protein phosphatase binding, phosphatase binding, ATPase activity (Figure 5C).

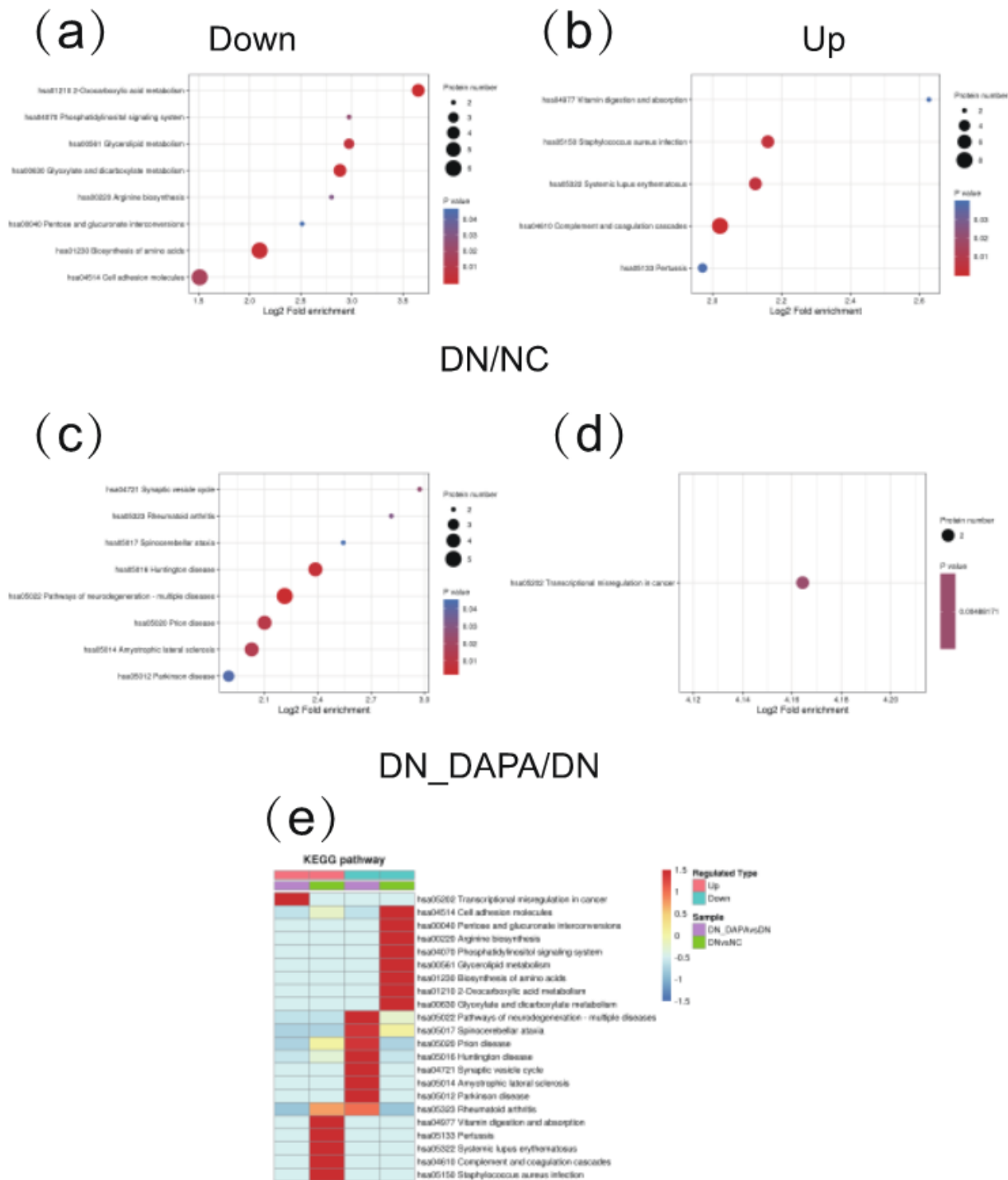


Figure 6

Enrichment analysis and clustering analysis of KEGG pathway involved in differential proteins in DN/NC and DN-DAPA/DN groups.

A: Enrichment analysis of KEGG pathway involved in differential proteins down-regulated in DN/NC group. B: Enrichment analysis of KEGG pathway involved in differential proteins up-regulated in DN/NC group. C: Enrichment analysis of KEGG pathway involved in differential proteins down-regulated in DN-DAPA/DN

group. D: Enrichment analysis of KEGG pathway involved in differential proteins up-regulated in DN-DAPA/DN group. E: Enrichment analysis of differential proteins involved in the clustering analysis of the KEGG pathway.